

Title	Nanostructured thermally sprayed cemented carbide layer fabricated by friction stir processing
Author(s)	Morisada, Yoshiaki; Fujii, Hidetoshi
Citation	Transactions of JWRI. 2011, 40(1), p. 35-39
Version Type	VoR
URL	https://doi.org/10.18910/6382
rights	
Note	

Osaka University Knowledge Archive : OUKA

<https://ir.library.osaka-u.ac.jp/>

Osaka University

Nanostructured thermally sprayed cemented carbide layer fabricated by friction stir processing†

MORISADA Yoshiaki * and FUJII Hidetoshi **

Abstract

The modification of a thermally sprayed cemented carbide (WC-CrC-Ni) layer by friction stir processing (FSP) was studied. The cemented carbide layer was successfully modified using a sintered cemented carbide (WC-Co) tool. The defects in the cemented carbide layer disappeared and the hardness of the cemented carbide layer increased to ~2000 HV, which was about 1.5 times higher than that of the as-sprayed cemented carbide layer. Additionally, the cemented carbide layer was bonded to the SKD61 substrate by diffusion of the metallic elements and the distortion of the coating - substrate interface producing a mechanical interlocking effect.

KEY WORDS: (Friction stir processing), (Thermal spray), (Cemented carbide layer), (Structural refinement), (Hardness)

1. Introduction

Cemented carbide and related materials have superior mechanical properties attributed to the high hardness of the WC particles and excellent fracture toughness of the metallic binders, such as Co or Ni¹⁻⁴). Their applicable field is wide and they are used as the base metals for cutting tools, dies, molds, etc. However, W, Co, and Ni, which are the main compositional elements of the cemented carbide, are rare and expensive. The amount of these elements should be reduced for resource savings and cost reduction. Additionally, the shape and the size of the sintered cemented carbides are limited because of the equipment used for sintering. Therefore, a coating technique to form the sound cemented carbide layer with its original mechanical properties is desired. Although thermally sprayed coatings can produce the cemented carbide layer on a substrate, an as-sprayed cemented carbide layer contains many defects and its hardness is much lower than that of the sintered cemented carbide^{5,6}). The weak adherence between the cemented carbide layer and the substrate is also a serious problem for many applications. In the past decade, laser heating treatment of the thermally sprayed layer has been studied to increase its mechanical properties^{7,8}). The laser heating treatment can eliminate the defects in the thermally sprayed cemented carbide layer and the hardness is increased by about 30 %⁹). However, the hardness shows a non-uniform distribution in the depth direction of the cemented carbide layer and it is still lower than that of

the sintered cemented carbide.

Recently, much attention has been paid to Friction Stir Processing (FSP) which is a surface modification technique for various metallic materials¹⁰⁻¹⁴). The principle of FSP is almost the same as Friction Stir Welding (FSW). A selected area of a metal plate can be modified by a rotating tool which is inserted into the metal plate, hence producing a plastically deformed zone. In this study, the modification of the thermally sprayed cemented carbide (WC-CrC-Ni) layer by FSP is investigated in order to improve the mechanical properties and enhance their applicable fields.

2. Experimental

2.1 Thermal spray of WC-CrC-Ni powder

Commercially available WC-20mass%CrC-7mass%Ni agglomerated powder (mean powder size: 40 μ m, Sumitomo Metal Mining Co., Ltd.) was sprayed onto an SKD61 (Nominal composition: 0.35-0.42 mass% C, 0.8-1.2 mass% Si, 0.25-0.5 mass% Mn, 4.8-5.5 mass% Cr, 1.0-1.5 mass% Mo, 0.8-1.2 mass% V, balance Fe) substrate (17 mm \times 175 mm \times 230 mm) by JP5000 HVOF thermal spraying equipment (Eutectic of Japan, Ltd.). The carrier gas, gun speed, and fuel were Ar, 3 mm/min, and coal oil (Nominal composition: methanol 1.1 mass%, ethanol 3.1 mass%, methyl t-butyl ether 6.9 mass%, paraffin hydrocarbon 31.1 mass%, naphthenic hydrocarbon 1.7 mass%, olefin hydrocarbon 12.3 mass%, aromatic hydrocarbon 43.8 mass%, oxygen 2.9 mass%),

† Received on June 10, 2011

* Assistant professor

** Professor

Transactions of JWRI is published by Joining and Welding Research Institute, Osaka University, Ibaraki, Osaka 567-0047, Japan

respectively. The thickness of the thermally sprayed cemented carbide layer was about 300 μ m.

2.2 FSP on the thermally sprayed WC-CrC-Ni layer

The thermally sprayed cemented carbide layer was modified by the FSP. The FSP tool made of sintered WC-Co cemented carbide and had a columnar shape (ϕ 12 mm) without a probe¹⁵. The bottom face of the FSP tool was flat. A constant tool rotating rate of 600 rpm was used and the constant travel speed was 50 mm/min. A tool tilt angle of 3° was used.

2.3 Evaluation of the as-sprayed and the FSP treated WC-CrC-Ni layer

Transverse sections of the as-sprayed and the FSP treated samples were mounted and then mechanically polished. The microstructure of the WC-CrC-Ni layer and the substrate were observed by optical microscopy and SEM (JEOL JSM-6460LA). The distribution of nanometer-sized defects and the microstructure of the metallic binder were evaluated by TEM (JEOL JEM-4000EX) at the accelerating voltage of 400 kV. The specimens for the TEM observations were prepared by FIB (Hitachi High-Technologies Corporation, FB-2000A). The boundary condition between the WC-CrC-Ni layer and the substrate was observed by SEM-EDS (JEOL JSM-6460LA, JED-2300). The crystal structures of the WC-CrC-Ni layer were identified by XRD (Rigaku RINT2500V). The microhardness was measured using a micro-vickers hardness tester (Akashi HM-124) with a load of 2.9 N. The fracture toughness was evaluated by the IF method with a load of 490 N.

3. Results and Discussion

3.1 Microstructure

The cross sectional SEM images of the as-sprayed sample are shown in **Fig. 1**. The WC-CrC-Ni layer of about 300 μ m in thickness formed on the SKD61 substrate could be confirmed. Although there was no macroscopic defect, such as exfoliation of the WC-CrC-Ni layer from the substrate or large cracks, the WC-CrC-Ni layer contained many small defects as shown in Fig. 1(b). **Figure 2** shows the cross sectional OM image of the FSP treated sample which was etched in 3 % nital. The thickness of the WC-CrC-Ni layer decreased from 300 μ m to 100~200 μ m due to the pressure and the stirring during the FSP. A stir zone (SZ) of about 550 μ m thick was formed on the substrate under the WC-CrC-Ni layer. The WC-CrC-Ni layer was not mixed with the substrate because the FSP by the non-threaded tool generated only horizontal plastic flows. The heat affected zone (HAZ), which was formed by the heat input during the FSP, could be confirmed under the SZ. **Figure 3** shows the microstructures of the FSP treated sample. The porosities in the WC-CrC-Ni layer disappeared due to the FSP. Additionally, the WC particles were densely packed as shown in Fig. 3(a). It is considered that the plastic flow of the Ni binder induced by the FSP led to the rearrangement of the WC particles. The SZ consisted of

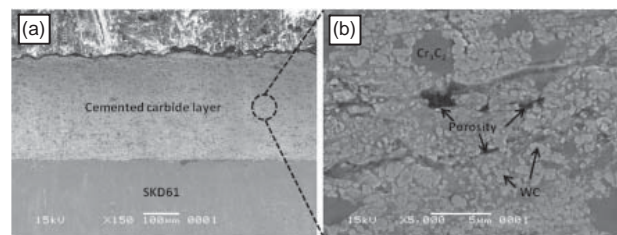


Fig. 1 SEM images of cross section of the as-sprayed sample.

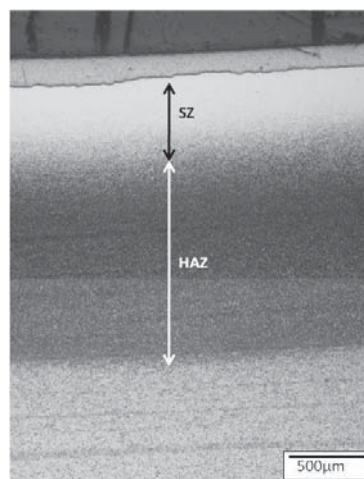


Fig. 2 OM image of cross section of the FSP treated sample.

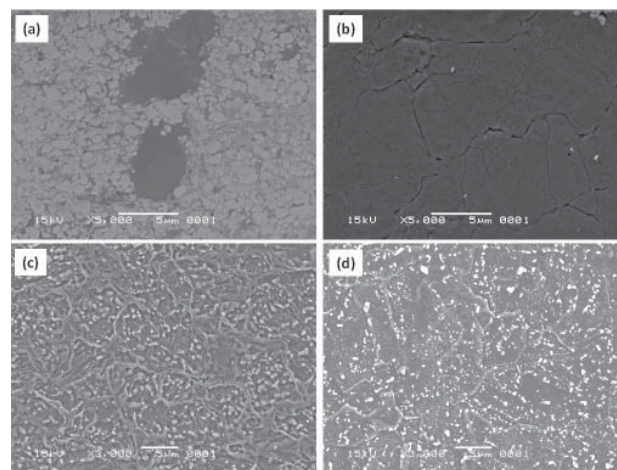


Fig. 3 Microstructures of the FSP treated sample. (a) WC-CrC-Ni layer, (b) SZ of SKD61, (c) HAZ of SKD61, and (d) untreated SKD61.

very fine martensite. The prior austenite grain was refined by the severe plastic deformation during the FSP and it was transformed to the martensite by quenching due to the tool travel. There were no crystallized chromium carbide particles on the SZ because they were dissolved into the matrix. It seems that the stirring by the tool accelerated the dissolution of the chromium carbide into the matrix at the processing temperature. The solution

heat treatment of the SKD61 led to the grain growth of the austenite. However, the microstructure of the SZ was finer than that of the as-received SKD61. On the other hand, the HAZ had the normal hardened structure of the SKD61 which indicated that this zone was not influenced by the severe plastic deformation.

TEM images of the WC-CrC-Ni layer at low magnification are shown in Fig. 4. Although many small pores could be confirmed in the as-sprayed layer, there were no pores in the FSP treated layer. Additionally, the filling density of the WC particles was clearly increased by the FSP. The Cr₃C₂ particles were fragmented and deformed by the tool and were dispersed in the matrix as shown in Fig. 4(b). A TEM image of the FSP treated WC-CrC-Ni layer at high magnification showed that the microstructure of the FSP treated Ni binder was refined on a nanometer order (Fig.5). It is considered that Ni was recrystallized by the severe plastic deformation during the FSP.

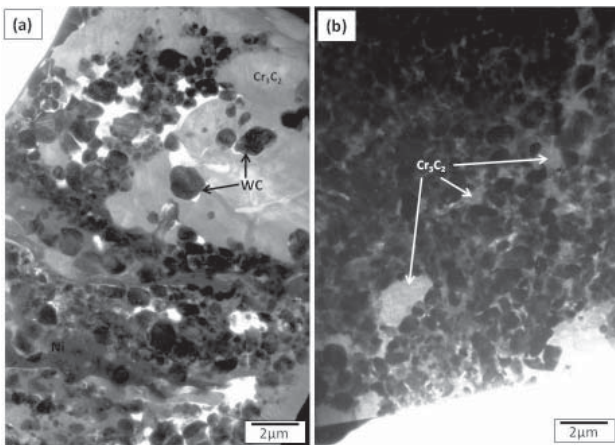


Fig. 4 TEM images of (a) as-sprayed WC-CrC-Ni layer and (b) FSP treated WC-CrC-Ni layer.

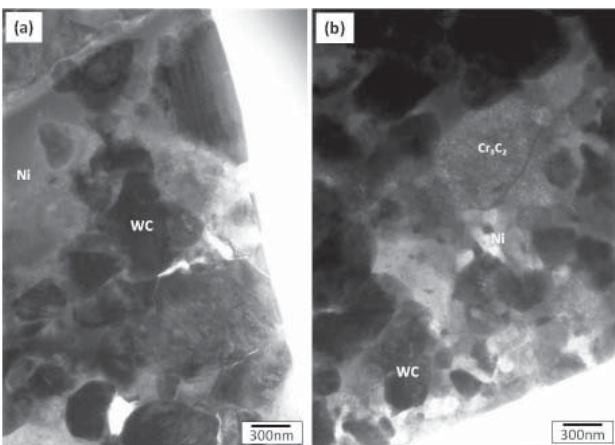


Fig. 5 Microstructures of the Ni binder for (a) as-sprayed WC-CrC-Ni layer and (b) FSP treated WC-CrC-Ni layer.

Figure 6 shows XRD patterns of the as-sprayed and the FSP treated WC-CrC-Ni layer. It can be found that they consisted of WC, Cr₃C₂, and a small amount of Ni. The peaks attributed to WC were not changed by the FSP. On the other hand, the peak intensity of Cr₃C₂ was increased by the FSP. The volume content of Cr₃C₂ in the measured area would be increased due to the dispersion of the fragmented and deformed Cr₃C₂ particles near the surface.

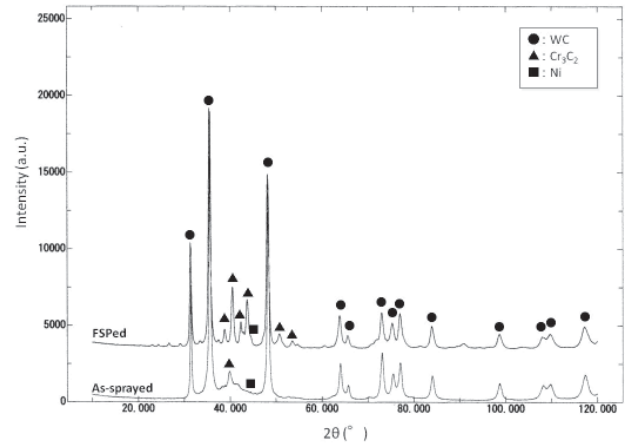


Fig. 6 XRD patterns of the as-sprayed and the FSP treated WC-CrC-Ni layer.

3.2 Mechanical properties

The microhardness horizontal profiles for the as-sprayed and the FSP treated WC-CrC-Ni layer are shown in Fig. 7. The microhardness at 100 µm from the surface was measured for the horizontal profile. The average microhardness of the as-sprayed WC-CrC-Ni layer was about 1200 HV which was similar to that of the

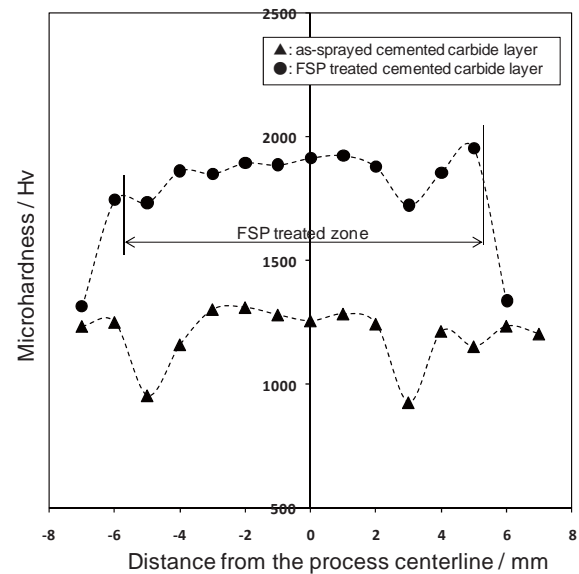


Fig. 7 Microhardness horizontal profiles of the cross-section of the as-sprayed and the FSP treated WC-CrC-Ni layer.

Nanostructured thermally sprayed cemented carbide layer fabricated by friction stir processing

thermally sprayed WC-CrC-Ni layer reported by other researchers⁹). The microhardness of the FSP treated zone reached ~ 2000 HV. Generally, the hardness of the cemented carbide was increased by the reduction of the metallic binder content and close to that of the monolithic WC. The obtained microhardness of 2000 HV was nearly the same value as that of the sintered WC. It should be mentioned that the microhardness of the FSP treated zone was higher than that of the sintered cemented carbide with the same chemical composition. It is difficult to explain such a large increase in the microhardness by only the elimination of the defects in the WC-CrC-Ni layer. It is considered that the grain refinement of the Ni binder and the rearrangement of the WC particles assisted in the change of the microhardness. The improvement of the mechanical properties of the cemented carbide has been studied by the decrease in the grain size of the WC particles¹⁶). For example, the spark plasma sintered WC-Co with the WC particles of ~ 100 nm and the hot pressed WC-Co with the WC particles of 169 nm had values of 1887 and 2084 HV, respectively^{17, 18}). On the other hand, there was no effective process to refine the microstructure of the metallic binder in the cemented carbide. Although the grain of the metallic materials could be refined by the recrystallization process, it was difficult for the cemented carbides because of their high deformation resistance. In this study, the plastic flow was successfully induced into the WC-CrC-Ni layer using the rotating tool made of WC-Co. **Figure 8** shows the microhardness depth profiles of the cross-section of the as-sprayed and the FSP treated WC-CrC-Ni layer. The microhardness of the substrate under the FSP treated WC-CrC-Ni layer had extremely high values of ~ 900 HV compared with that of the normal hardened steel, SKD61 which was about 550 HV. It is considered that the fine martensite structure formed by the FSP and the solution of the chromium carbide led to such a high hardness. The gradual decrease in the microhardness under the WC-CrC-Ni layer had the advantage in being compatible with a high wear resistance and toughness.

Figure 9 shows the fracture toughness of the WC-CrC-Ni layer. It was measured by indentation fracture method and calculated by the following equation¹⁹).

$$K_{Ic} = 0.0515P/C^{3/2}$$

where P is the indentation load (N), and C is the surface crack length (m). The fracture toughness of the as-sprayed WC-CrC-Ni layer was $6.2 \text{ MPa} \cdot \text{m}^{1/2}$ and that of the FSP treated WC-CrC-Ni layer was $6.5 \text{ MPa} \cdot \text{m}^{1/2}$, respectively. Although the microhardness was increased by the FSP, the fracture toughness was not decreased. It seems that the crack propagated along the boundary of the lamellar structure for the as-sprayed WC-CrC-Ni layer. Therefore, the width of the crack was large. On the other hand, the crack propagation of the FSP treated WC-CrC-Ni layer was not affected by the original lamellar structure of the as-sprayed WC-CrC-Ni layer. It is considered that the bonding strength between the WC-CrC-Ni agglomerated powders was increased by the

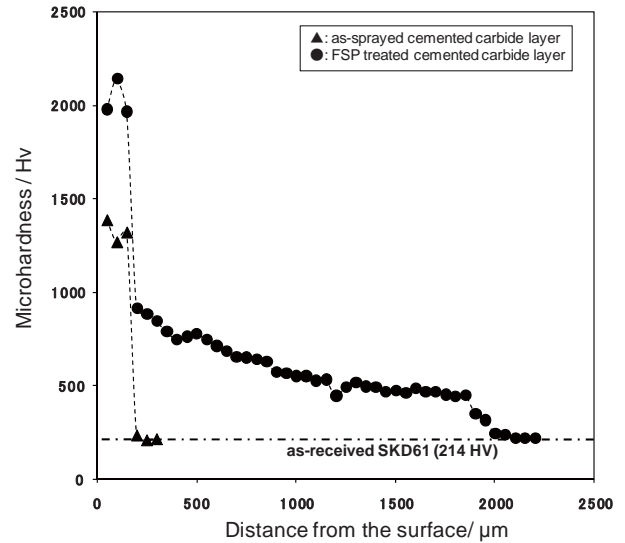


Fig. 8 Microhardness depth profiles of the cross-section of the as-sprayed and the FSP treated WC-CrC-Ni layer.

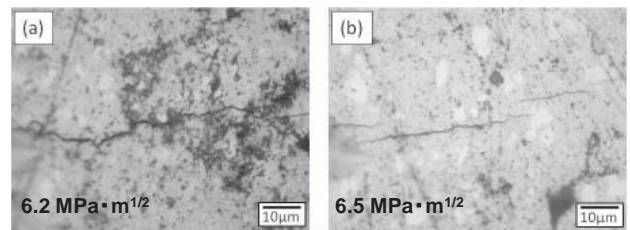


Fig. 9 Crack propagations by the indentation fracture test. (a) as-sprayed WC-CrC-Ni layer and (b) FSP treated WC-CrC-Ni layer.

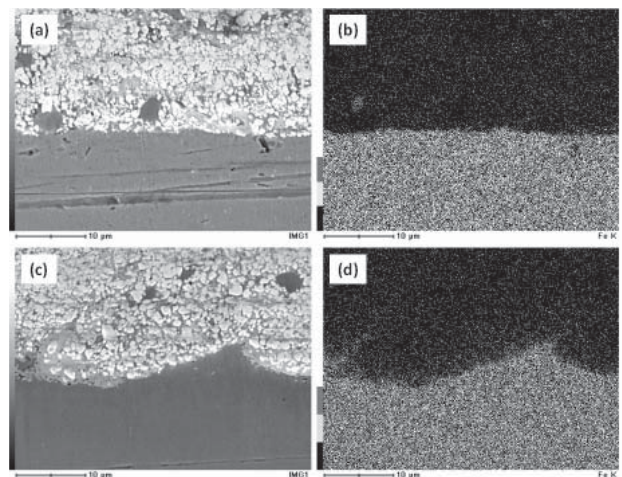


Fig. 10 SEM images and Fe mapping images of the boundary between the WC-CrC-Ni layer and the substrate. (a) SEM image of the as-sprayed sample, (b) SEM image of the FSP treated sample, (c) Fe mapping image of the as-sprayed sample, and (d) Fe mapping image of the FSP treated sample.

FSP. Additionally, the FSP treated WC-CrC-Ni layer and the substrate were tightly connected by the diffusion of the metallic elements and the distortion of the coating - substrate interface producing a mechanical interlocking effect. The diffusion of Fe into the WC-CrC-Ni layer and the undulating boundary could be confirmed for the FSP treated sample as shown in Fig. 10.

4. Conclusions

- (1) The thermally sprayed WC-CrC-Ni layer was successfully modified by the FSP. The obtained results are summarized as follows.
- (2) The WC-CrC-Ni layer and the SKD61 substrate can be stirred by the rotating tool made of WC-Co. The defects in the WC-CrC-Ni layer disappear and the WC particles are closely packed after the FSP.
- (3) The Ni binder and the Cr₃C₂ particles in the WC-CrC-Ni layer are refined by the FSP.
- (4) The FSP treated WC-CrC-Ni layer has an extremely high microhardness of ~2000 HV which is higher than that of the sintered cemented carbide with the same composition.
- (5) The FSP treated WC-CrC-Ni layer and the substrate are tightly connected by the diffusion of the metallic elements and the distortion of the coating - substrate interface producing a mechanical interlocking effect.

References

- 1) S. Mi and T.H. Courtney, *Scripta Mater.* 38 (1997) 171-176.
- 2) G.S. Upadhyaya, *Materials and Design* 22 (2001) 483-489.
- 3) Y. Morisada and Y. Miyamoto, *Mater. Sci. Eng. A* 381 (2004) 58-62.
- 4) Y. Miyamoto, Y. Morisada, H. Moriguchi, K. Tsuduki, and A. Ikegaya, *Ceramic Trans.* 146 (2004) 393-399.
- 5) H.S. Ni, X.H. Liu, X.C. Chang, W.L. Hou, W. Liu, and J.Q. Wang, *J. Alloys Compd.* 467 (2009) 163-167.
- 6) T.Y. Cho, J.H. Yoon, K.S. Kim, K.O. Song, Y.K. Joo, W. Fang, and S.H. Zhang, *Surf. Coat. Technol.* 202 (2008) 5556-5559.
- 7) E. Cappelli, S. Orland, F. Pinzari, A. Napoli, and S. Kaciulis, *Appl. Surf. Sci.* 138-139 (1999) 376-382.
- 8) D. Triantafyllidis, L. Li, and F.H. Stott, *Surf. Coat. Technol.* 201 (2006) 3163-3173.
- 9) S.H. Zhang, T.Y. Cho, J.H. Yoon, M.X. Li, P.W. Shum, and S.C. Kwon, *Mater. Sci. Eng. B* 162 (2009) 127-134.
- 10) R.S. Mishra, Z.Y. Ma, and I. Charit, *Mater. Sci. Eng. A* 341 (2003) 307-310.
- 11) Y. Morisada, H. Fujii, T. Nagaoka, M. Fukusumi, *Scripta Mater* 55 (2006) 1067-1070.
- 12) Y. Morisada, H. Fujii, T. Nagaoka, M. Fukusumi, *Mater Sci Eng A* 419 (2006) 344-348.
- 13) Y. Morisada, H. Fujii, T. Nagaoka, K. Nogi, and M. Fukusumi, *Composites A*, 38 (2007) 2097-2101.
- 14) Y. Morisada, H. Fujii, T. Mizuno, G. Abe, T. Nagaoka, and M. Fukusumi, *Surf. Coat. Technol.* 204 (2009) 386-390.
- 15) H. Fujii, L. Cui, N. Tsuji, M. Maeda, K. Nakata and K. Nogi, *Mater.Sci. Eng. A*429 (2006) 50-57.
- 16) Z.Z. Fang, X. Wang, T. Ryu, K.S. Hwang, and H.Y. Sohn, *Int. J. Refract. Metals and Hard Mater.* 27 (2009) 288-299.
- 17) L.H. Zhu, Q.W. Huang, and H.F. Zhao, *J. Mater. Sci. Lett.* 22 (2003) 1631-1633.
- 18) C.G. Lin, E. Kny, G.S. Yuan, and B. Djuricic, *J. Alloys Compd.* 383 (2004) 98-102.
- 19) H.R. Lawn and E.R. Fuller, *J. Mater. Sci.* 10 (1975) 2014-2024.